The renal thiazide-sensitive Na-Cl cotransporter as mediator of the aldosterone-escape phenomenon

Xiao-Yan Wang,[1] Shyama Masilamani,[1] Jakob Nielsen,[1] Tae-Hwan Kwon,[2] Heddwen L. Brooks,[1] Søren Nielsen,[2] and Mark A. Knepper[1]

[1]Laboratory of Kidney and Electrolyte Metabolism, National Heart, Lung and Blood Institute, National Institutes of Health, Bethesda, Maryland, USA
[2]Department of Cell Biology, Institute of Anatomy, University of Aarhus, Aarhus, Denmark

Address correspondence to: Mark A. Knepper, National Institutes of Health, Building 10, Room 6N260, 10 Center Drive MSC 1603, Bethesda, Maryland 20892-1603, USA.
Phone: (301) 496-3064; Fax: (301) 402-1443; E-mail: knep@helix.nih.gov.

Received for publication May 18, 2000, and accepted in revised form June 4, 2001.

The kidneys "escape" from the Na-retaining effects of aldosterone when circulating levels of aldosterone are inappropriately elevated in the setting of normal or expanded extracellular fluid volume, e.g., in primary aldosteronism. Using a targeted proteomics approach, we screened renal protein extracts with rabbit polyclonal antibodies directed to each of the major Na transporters expressed along the nephron to determine whether escape from aldosterone-mediated Na retention is associated with decreased abundance of one or more of renal Na transporters. The analysis revealed that the renal abundance of the thiazide-sensitive Na-Cl cotransporter (NCC) was profoundly and selectively decreased. None of the other apical solute-coupled Na transporters displayed decreases in abundance, nor were the total abundances of the three ENaC subunits significantly altered. Immunocytochemistry showed a strong decrease in NCC labeling in distal convoluted tubules of aldosterone-escape rats with no change in the cellular distribution of NCC. Ribonuclease protection assays (RPAs) revealed that the decrease in NCC protein abundance was not associated with altered NCC mRNA abundance. Thus, the thiazide-sensitive Na-Cl cotransporter of the distal convoluted tubule appears to be the chief molecular target for regulatory processes responsible for mineralocorticoid escape, decreasing in abundance via a posttranscriptional mechanism.

J. Clin. Invest. **108**:215–222 (2001). DOI:10.1172/JCI200110366.

Introduction

Regulation of extracellular fluid volume and blood pressure depends largely on control of Na excretion by the kidney. One of the major regulators of Na excretion is aldosterone. Aldosterone is an adrenocortical steroid hormone whose actions are mediated chiefly by binding to intracellular receptors that function as transcription factors in the activated state (1). Aldosterone stimulates Na retention by the kidney in part through its action to regulate the epithelial Na channel, ENaC, which mediates apical Na entry across collecting duct principal cells (2). ENaC is a hetero-oligomeric channel made up of three distinct subunits (3). We have recently demonstrated that the action of aldosterone is associated with a large increase in the protein abundance of the α subunit of ENaC and a molecular weight shift of the γ subunit from 85 to 70 kDa, possibly owing to physiological proteolytic cleavage (4). In addition, aldosterone stimulates Na reabsorption in the distal convoluted tubule (DCT; ref. 5), by increasing the abundance of the thiazide-sensitive Na-Cl cotransporter (NCC) in the DCT (6). Thus, both NCC and ENaC appear to be primary targets for regulation of sodium excretion by aldosterone.

The effect of aldosterone to cause renal Na retention can be overridden in some circumstances by the phenomenon of aldosterone escape (7, 8). Aldosterone escape is a manifestation of the ability of the kidney to overcome the Na-retaining effects of aldosterone when aldosterone levels are high despite an Na-replete state. This phenomenon may be important clinically, for example, in primary aldosteronism (9), in which it may ameliorate the hypertensive effects of high circulating levels of aldosterone.

Aldosterone escape is dependent on increased renal vascular perfusion pressure rather than systemic factors such as changes in circulating hormone levels or renal nerve activity (10). Thus, the aldosterone-escape process appears to be a manifestation of the long-term pressure natriuresis phenomenon, which plays a central role in long-term regulation of systemic blood pressure. The increase in Na excretion in aldosterone escape occurs without an increase in glomerular filtration rate, implicating decreased renal tubule Na reabsorption (11, 12). Micropuncture measurements demonstrated increased Na delivery to the collecting duct (11, 12). However, the specific site of decreased Na reabsorption has not been identified, and the Na transporters involved remain unknown. In this study, we use a "targeted-proteomics" approach (13) in rats to look for renal Na transporters downregulated in aldosterone escape. This approach

uses a battery of antibodies to each of the major renal tubule Na transporters to screen renal homogenates for downregulated transporters.

Methods

Aldosterone-escape model. Experiments were conducted in male Sprague-Dawley rats (180–220 g) (Taconic Farms, Germantown, New York, USA). The aldosterone-escape protocol is diagrammed in Figure 1. All rats were maintained in metabolism cages to allow quantitative urine collections. On day –3, all rats were anesthetized with methoxyflurane (Metofane; Pitman-Moore, Mundelein, Illinois, USA) and implanted subcutaneously with osmotic minipumps (model 2ML2; Alzet, Palo Alto, California, USA) delivering 200 μg per day of aldosterone (Sigma Chemical Co., St. Louis, Missouri, USA) (6). The minipump infusion was sustained throughout the entire time course of each experiment in all rats. The intake of Na was initially maintained at a very low level (0.02 mEq/d) by ration feeding of measured amounts of a gelled mixture of low-Na food and water (see below). On day 0 (see Figure 1), half the rats were switched to a higher Na intake (2.0 mEq/d), whereas the remaining rats were continued on the 0.02 mEq/d Na intake. The rats given the higher Na intake must escape from the Na-retaining effect of aldosterone to re-establish Na balance.

Kidneys were analyzed at various time points after the switch from 0.02 to 2.0 mEq/d Na to determine Na transporter and Na channel abundance as described below. The low-Na control rats were handled in a manner identical to the experimental rats throughout the time course, including matched caloric and water intake achieved by ration feeding (see below). Rats were euthanized by decapitation. Serum was collected at the time of decapitation for the measurement of aldosterone concentration by RIA (Coat-a-Count; Diagnostic Products Corp., Los Angeles, California, USA), Na concentration, and creatinine concentration (Monarch 2000 autoanalyzer; Instrumentation Laboratories, Lexington, Massachusetts, USA). Urinary samples were analyzed for Na and creatinine (Monarch 2000 autoanalyzer).

Ration feeding protocol. The intakes of sodium, calories, and water were carefully controlled by ration feeding of a fixed daily amount of a gelled diet that contains all of the nutrients, NaCl, and water that the rat receives in a day (6). The baseline low Na intake was achieved by feeding the rats a gelled mixture of a synthetic low-Na diet (Formula 53140000; Ziegler Brothers, Gardner, Pennsylvania, USA), deionized water (25 ml per 15 g of food), and agar (0.125 g per 25 ml of water). The Na-replete diet was the same except for addition of 2 mEq Na per 15 g of food before gelation. All animals received the equivalent of 15 g per 200 g of body weight (BW) per day of rat chow determined by weighing the gelled mixture. Analysis of the diet demonstrated that this protocol provides approximately 0.02 mEq per 200 g of BW per day of Na for the low-Na mixture and 2.0 mEq per 200 of g BW per day for the Na-replete diet.

Antibodies. Rabbit polyclonal antibodies to the following renal sodium transporters were utilized: the type 2 Na-phosphate cotransporter (NaPi-2) of the proximal tubule (14), the type 3 Na-H exchanger (NHE3) of the proximal tubule (15), the Na-K-2Cl cotransporter (NKCC2) of the thick ascending limb (16), the thiazide-sensitive Na-Cl cotransporter (NCC) of the DCT (6), and all three subunits of the epithelial Na channel (ENaC) of the collecting duct (4). The antisera were affinity purified against the immunizing peptides as described previously (6, 16). Specificity of the antibodies has been demonstrated by showing unique peptide-ablatable bands on immunoblots and a unique distribution of labeling by immunocytochemistry. In addition, we utilized a mouse mAb against the Na-K-ATPase α1 subunit (product number 05-369; Upstate Biotechnology Inc., Lake Placid, New York, USA).

Semiquantitative immunoblotting. Semiquantitative immunoblotting was used to compare sodium transporter or channel abundance between groups of rats as described in detail previously (13, 16, 17). The left kidneys were homogenized intact. The right kidneys were dissected to obtain cortex, inner stripe of outer medulla, and inner medulla. For each set of samples (experimental and control), after solubilization in Laemmli sample buffer, an initial gel was stained with Coomassie Blue as described previously (18) to confirm equal loading among samples. SDS-PAGE was performed on 7.5%, 10%, or 12% polyacrylamide gels (Ready Gels; Bio-Rad Laboratories Inc., Hercules, California, USA), and the proteins were transferred from the gel electrophoretically to nitrocellulose membranes. Membranes were probed overnight at 4°C with the respective primary antibodies and then exposed to secondary antibody (goat anti-rabbit IgG conjugated with horseradish per-

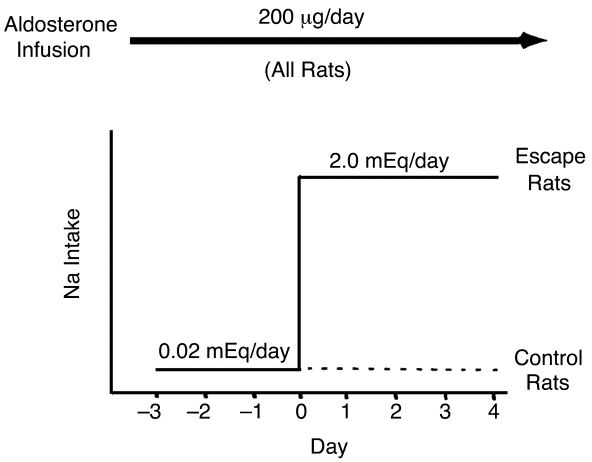

Figure 1
Diagram of aldosterone-escape protocol. All rats received aldosterone infusions by osmotic minipump (top). Both control and escape rats were started at day –3 on a low-Na diet providing approximately 0.02 mEq/d of Na. On day 0, the Na intake was increased to 2.0 mEq/d for the escape rats, whereas control rats continued to receive 0.02 mEq/d.

oxidase, no. 31463, diluted to 1:5,000; or rabbit anti-mouse IgG conjugated with horseradish peroxidase, no. 31450, diluted to 1:5,000; both from Pierce Chemical Co., Rockford, Illinois, USA) for 1 hour at room temperature. Sites of antibody-antigen reaction were visualized using a luminol-based enhanced chemiluminescence substrate (LumiGLO; Kirkegaard and Perry Laboratories, Gaithersburg, Maryland, USA) before exposure to X-ray film (Kodak 165-1579; Eastman Kodak Co., Rochester, New York, USA). The band densities were quantitated by laser densitometry (Model PDS1-P90; Molecular Dynamics Inc., Sunnyvale, California, USA). The densitometry values were normalized to facilitate comparisons.

Immunocytochemistry. Control (n = 3) and aldosterone-escape (n = 3) rats were prepared as described above. The kidneys were fixed by perfusion with cold PBS (pH 7.4) for 15 seconds via the abdominal aorta followed by cold 4% paraformaldehyde in 0.1M cacodylate buffer (pH 7.4) for 3 minutes. The kidneys were removed and post-fixed for 1 hour, followed by three 10-minute washes with 0.1M cacodylate buffer (pH 7.4). The tissue was dehydrated in graded ethanol and left overnight in xylene. The tissue was embedded in paraffin, and 2-μm sections were cut on a rotary microtome (Leica, Herlev, Denmark). Localization of NCC was carried out using indirect immunofluorescence or immunoperoxidase labeling as described elsewhere (19). The primary antibody was rabbit anti-rat NCC L573 (6). For confocal microscopy, the secondary antibody was Alexa 488 conjugated goat anti-rabbit IgG antibody (A-11008; Molecular Probes Inc., Eugene, Oregon, USA). For immunoperoxidase labeling, the secondary antibody was horseradish peroxidase conjugated to goat anti-rabbit IgG (P448; DAKO A/S, Glostrup, Denmark). For immunoperoxidase labeling, counterstaining was done using Mayer's hematoxylin. Microscopy was carried out with Leica DMRE light microscope (Leica, Herlev, Denmark) and a Zeiss LSM510 laser confocal microscope (Brock & Michelsen, Birherød, Denmark).

In some of the immunofluorescence studies, double labeling was carried out using the mAb to the Na-K-ATPase α-1 subunit (see above) with a goat anti-mouse secondary antibody conjugated to Alexa 546 (A11003; Molecular Probes Inc.).

RNA preparation. Total kidney RNA was extracted from the right kidneys of control and aldosterone-escape rats treated as described previously (20) using *RNAzol B* (Tel-Test Inc., Friendswood, Texas, USA). RNA purity and concentration were assessed spectrophotometrically. RNA integrity was confirmed by inspection of ribosomal RNA bands on ethidium bromide–stained agarose gels.

RNA probe synthesis. The DNA template for the synthesis of the NCC RPA probe was generated by PCR from rat kidney cDNA using the following primers: NCC Forward primer 5′-CCT GCT GTG TCA TCA CAT C-3′, and NCC T7 Reverse primer: 5′-GCG CGT AAT ACG ACT CAC TAT AGG GAG AGG AGT TAA GGG AAC AGG AGG AGA AAT G-3′. The reverse primer (antisense primer) was made with the T7 sequence incorporated at the 5′-end of the PCR primer. The PCR product was used as the template without cloning it. The DNA template for the β-actin probe was provided by the manufacturer (7794; Ambion Inc., Austin, Texas, USA). Biotin-labeled antisense RNA probes for NCC and β-actin were synthesized from the templates with the MEGAscript kit (Ambion Inc.). The product was excised from 10% acrylamide SDS-PAGE gel following visualization with thin layer chromotography ultraviolet shadowing plates, and was eluted using the manufacturer's buffer (414; Ambion Inc.).

RPA. The RPA was carried out using an RPA assay kit (RPA III, 1414; Ambion Inc.) according to the protocol recommended by the manufacturer. Solution hybridization was performed with 10 μg total RNA samples from control and aldosterone-escape kidneys using the biotin-labeled antisense RNA probes for NCC (1 ng per tube) and β-actin (10 ng per tube). The hybridization was carried out at 56°C. After ribonuclease digestion, the products were denatured by heating to 94°C for 4 minutes and run on a urea-TBE polyacrylamide gel (5% polyacrylamide) and transferred to nylon membranes. The products were visualized by incubation of the membranes with an alkaline phosphatase/streptavidin probe and incubation with a chemiluminescence reagent (Bright-Star; Ambion Inc.) followed by exposure to light-sensitive film (BioMax Light, double coated; Kodak). Band densities were assessed by densitometry (PDS1-P90; Molecular Dynamics Inc.). Positive and negative controls were run with the probe alone (plus yeast RNA), with and without digestion.

Presentation of data and statistical analyses. Statistical comparisons were accomplished by unpaired t test (when variances were the same) or by Mann-Whitney rank-sum test (when variances were significantly different between groups). P values less than 0.05 were considered statistically significant.

Table 1
BW, serum aldosterone, creatinine clearance, water excretion, and Na excretion

	Control	Escape
n	5	5
BW (g), day –3	189.6 ± 4.5	189.0 ± 2.4
BW (g), day 0	193.8 ± 3.6	189.4 ± 3.9
BW (g), day 4	202.8 ± 3.9	198.6 ± 6.3
Serum aldosterone (nM)		
Day 4	56.7 ± 13.6	46.7 ± 13.9
Creatinine clearance (ml/h)		
Day 4	66.2 ± 3.4	64.6 ± 8.7
Water excretion (ml/d)		
Day 4	14.7 ± 1.0	12.1 ± 2.7
Na excretion (mEq/d)		
Day 4	0.1 ± 0.0	1.8 ± 0.3[A]
Urine Na concentration (mEq/l)		
Day 4	4.0 ± 0.0	155.2 ± 20.5[A]

[A]$P < 0.05$.

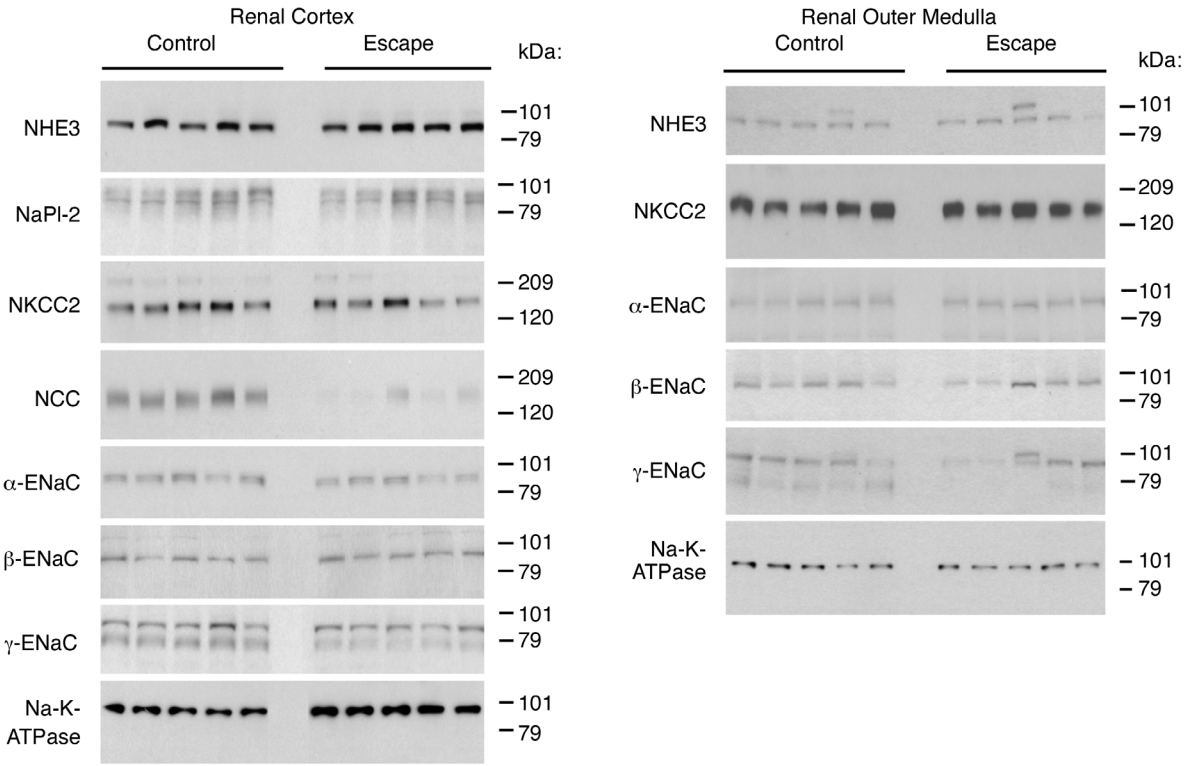

Figure 2
Immunoblots assessing Na transporter and Na channel abundances in homogenates from renal cortex (left) and renal outer medulla (right) in control (aldosterone-low Na) and escape (aldosterone-high Na) rats. Each lane was loaded with a sample from a different rat. Table 2 summarizes densitometric analysis.

Results

Aldosterone escape model. Figure 1 summarizes the aldosterone escape protocol. The escape phenomenon was elicited in aldosterone-infused rats by switching from a low to a high NaCl intake. Control rats received the same aldosterone infusion but were maintained on a low-NaCl intake and thus did not undergo escape. Table 1 shows data on BW, serum aldosterone concentration, creatinine clearance, water excretion rate, Na excretion rate, and urinary Na concentration in the initial set of rats studied. In the experimental group, the Na excretion rate rose virtually to the level of the intake, indicating that these rats successfully escaped from the Na-retaining action of aldosterone. The rise in Na excretion in the aldosterone-escape group occurred without a change in creatinine clearance, indicating that the increase in excretion was due to decreased renal tubule absorption.

Na transporter abundances in kidney. To determine whether the increase in Na excretion in the aldosterone-escape rats was associated with a decrease in the abundance of any of the major Na transporters expressed along the renal tubule, we screened renal homogenates using an ensemble of affinity-purified rabbit polyclonal antibodies. Figure 2 shows the initial results for renal cortex and outer medulla. Quantitative analysis of the data is shown in Table 2. In renal cortex, the major finding was a marked decrease in the abundance of NCC (the thiazide-sensitive cotransporter of the DCT) in aldosterone-escape rats. The NCC abundance fell to 17% ± 5% of the mean for the control rats (Table 2). The band densities corresponding to NHE3, NaPi-2, NKCC2, the α subunit of ENaC, and the β subunit of ENaC were not significantly changed in the aldosterone escape group compared with the aldosterone/low Na control rats. Although there was no change in the abundance of the 85-kDa form of γ-ENaC, there was a significant decrease in the abundance of the aldosterone-induced 70-kDa form, suggesting a partial reversal of

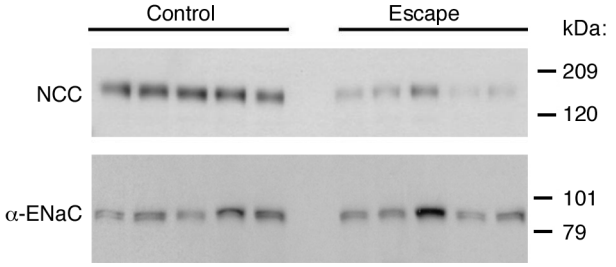

Figure 3
Immunoblots assessing NCC and α-ENaC abundances in homogenates from whole kidney in control (aldosterone/low Na) and escape (aldosterone/high Na) rats. Densitometric analysis revealed that only NCC abundance was decreased.

Table 2
Densitometric analysis of semiquantitative immunoblots of Na transporters and channels[A]

	Cortex		Outer medulla		Whole kidney	
	Control	Escape	Control	Escape	Control	Escape
NHE3	100 ± 11	142 ± 24	100 ± 5	91 ± 19	100 ± 9	139 ± 13[A]
NaPi2	100 ± 5	137 ± 18	Not expressed		100 ± 9	170 ± 26[A]
NKCC21	00 ± 17	77 ± 21	100 ± 20	86 ± 8	100 ± 20	79 ± 15
NCC	100 ± 18	17 ± 5[A]	Not expressed		100 ± 8	25 ± 7[A]
α-ENaC	100 ± 12	76 ± 10	100 ± 16	83 ± 17	100 ± 21	138 ± 24
β-ENaC	100 ± 14	77 ± 13	100 ± 13	106 ± 20	100 ± 21	145 ± 25
γ-ENaC						
85-kDa band	100 ± 15	79 ± 8	100 ± 16	69 ± 17	100 ± 28	143 ± 15
70-kDa band	100 ± 4	48 ± 5[A]	100 ± 9	35 ± 11[A]	100 ± 13	60 ± 10[A]
Na-K-ATPase						
α1 subunit	100 ± 9	196 ± 19[A]	100 ± 13	65 ± 10	100 ± 19	126 ± 36

Values are mean ± SE. [A]$P < 0.05$. All values are normalized by the mean for the control group and expressed as a percentage. ($n = 6$ for both control and escape groups.)

the effect of aldosterone on γ-ENaC (see Introduction). Interestingly, there was a significant increase in the abundance of the α-1 subunit of the Na-K-ATPase, a change that is unlikely to be related to the escape phenomenon because it would predict an increase in renal tubule Na absorption (see Discussion).

In outer medulla, the pattern of responses for NHE3, NKCC2, and the three subunits of ENaC was the same as in the cortex (Figure 2; Table 2). (Note that NCC and NaPi-2 are not expressed in inner stripe of outer medulla and therefore were not examined by immunoblotting in outer medullary samples.) In contrast to the cortex, Na-K-ATPase α-1 subunit abundance was not increased in outer medulla.

Figure 3 shows immunoblots for NCC and α-ENaC in whole-kidney samples from the same rats as shown in Figure 2. Once more, there was a marked suppression of the abundance of NCC (as seen in the cortical samples) to 25% ± 7% of the mean for the control rats, whereas α-ENaC abundance was not decreased (Table 2).

Immunocytochemistry. Figure 4 shows immunofluorescence labeling of NCC in the renal cortex of control and aldosterone-escape rats. Figure 4a shows double labeling using antibodies to the thiazide-sensitive cotransporter NCC (green) and the Na-K-ATPase (red). Labeling conditions and exposure settings on the confocal microscope were identical for the two images. As can be seen, the anti-NCC antibody labeled exclusively the apical membrane region of a subset of tubules recognized to be DCTs (21). The NCC labeling was decreased in the DCT cells from aldosterone-escape rats. The Na-K-ATPase labeling marks the basolateral plasma membrane domains in DCTs and other segments. The Na-K-ATPase labeling dominates the basal two thirds of the cells owing to the extensive basal infoldings of the DCT cells. Figure 4b shows a pair of low-power NCC immunofluorescence micrographs from control and aldosterone-escape rats. Labeling conditions and exposure settings on the confocal microscope were again identical for the two images. A relatively uniform decrease in NCC labeling in all DCTs can be appreciated. Similar observations were made in two additional pairs of rats.

Figure 5 shows similar sections labeled for NCC using immunoperoxidase techniques. The upper two panels show high-power images demonstrating a marked decrease in NCC labeling in aldosterone escape versus control. There was no obvious redistribution of NCC labeling in DCT cells. Lower-power images (bottom panels) show that the decrease in NCC occurs generally throughout the cortex. Similar observations were made in three pairs of rats. Thus, we conclude that the aldosterone-escape process is associated with a marked decrease in the abundance of NCC in the DCT cells, but that there is no marked change in the cellular distribution of NCC in these cells.

Time course of aldosterone escape. To determine whether the increase in Na excretion in aldosterone escape correlates with the demonstrated decreases in the abundance of NCC, we carried out time course studies using the protocol shown in Figure 1, and sampled rats at 1, 2, and 4 days after switching from the low-Na to the high-Na diet. Creatinine clearances (in milli-

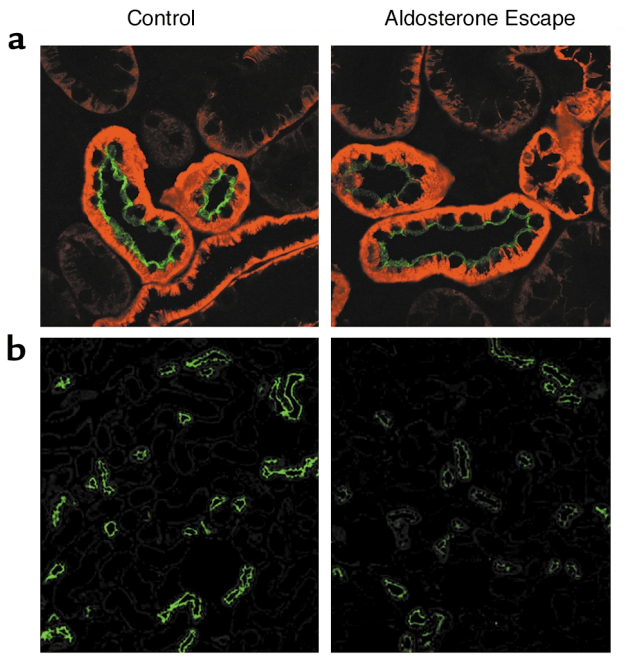

Figure 4
Confocal images showing immunofluorescence labeling of NCC in rat renal cortex. (**a**) Double labeling for NCC (green) and Na-K-ATPase α-1 subunit (red). ×250. (**b**) Low-power images of NCC labeling. ×40.

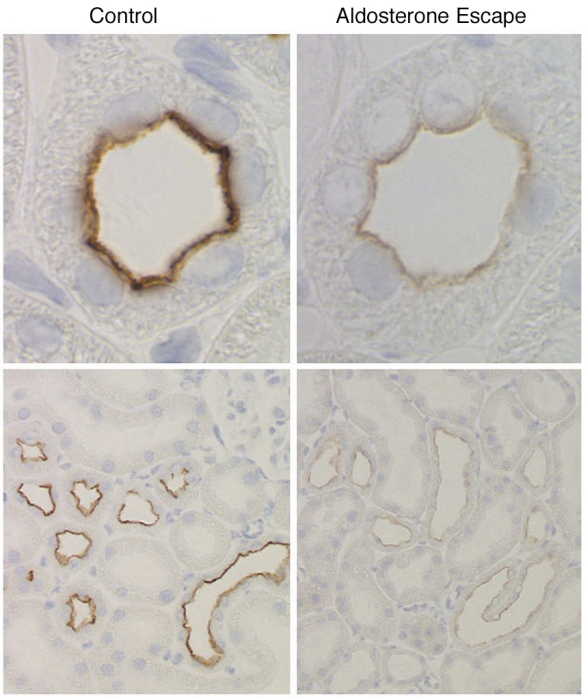

Figure 5
Immunoperoxidase NCC labeling in rat renal cortex of control and aldosterone-escape rats. Upper panels, ×625; lower panels, ×75.

liters per minute per 200 grams of BW) for the three time points were: day 1, control 0.83 ± 0.09, escape 0.73 ± 0.04 (NS); day 2, control 0.84 ± 0.07, escape 0.72 ± 0.04 (NS); day 4, control 1.10 ± 0.06, escape 1.08 ± 0.14 (NS). The time course of changes in NCC in renal cortex after increasing Na intake in the aldosterone escape protocol is shown in Figure 6. NCC abundance fell significantly in the first day after increasing Na intake, and the increase in Na excretion correlated with the decrease in NCC abundance.

NCC mRNA abundance. To assess whether the decrease in NCC protein abundance in the kidneys of aldosterone-escape rats is owing to a decrease in NCC mRNA, we assessed mRNA abundance by RPAs. As shown in the left panel of Figure 7, addition of increasing amounts of renal cortical mRNA results in a progressive increase in band density for both NCC and β-actin, illustrating that the assay is capable of detecting changes in mRNA abundance when loaded with 2–18 μg per tube. The right panel shows an absence of a difference in NCC mRNA levels between control and aldosterone-escape rats. In three such pairs of rats, there was no change in band densities for NCC mRNA (normalized to β-actin): control, 0.27 ± 0.02; aldosterone-escape, 0.27 ± 0.05 (no significant difference). Immunoblots using homogenates from the opposite kidneys of these rats confirmed that NCC protein abundance was markedly decreased (data not shown). Thus, the decrease in NCC abundance in aldosterone escape does not depend on a decrease in NCC mRNA levels.

Discussion

Experimental strategy. The major apical Na transporters responsible for Na absorption along the nephron were originally characterized by a combination of isolated perfused tubule studies, micropuncture studies, and studies of proximal tubule brush border vesicles, chiefly in the 1970s and 1980s. The evidence from these studies was instrumental in the eventual cloning of cDNAs for these transporters. These cDNA sequences have now enabled us to produce an ensemble of affinity-purified, peptide-directed rabbit polyclonal antibodies to each of the major apical Na transporters and channels expressed along the nephron (4, 6, 14–16, 22). The approach used here (a so-called targeted proteomics approach; ref. 13) is to employ the entire ensemble of antibodies to screen kidney homogenates from rats undergoing mineralocorticoid escape versus control rats to determine whether the escape phenomenon is associated with altered abundance of any of the major apical Na transporters. To determine relative abundance of each transporter (versus control), we use a semiquantitative immunoblotting protocol previously developed for the study of regulation of renal aquaporins (17). We emphasize that this technique will only detect regulatory processes that result in changes in transporter protein abundance or molecular weight. Detection of other modes of regulation such as transporter trafficking and phosphorylation will require different methods.

The experimental protocol in rats (Figure 1) was designed to separate the primary effects of aldosterone

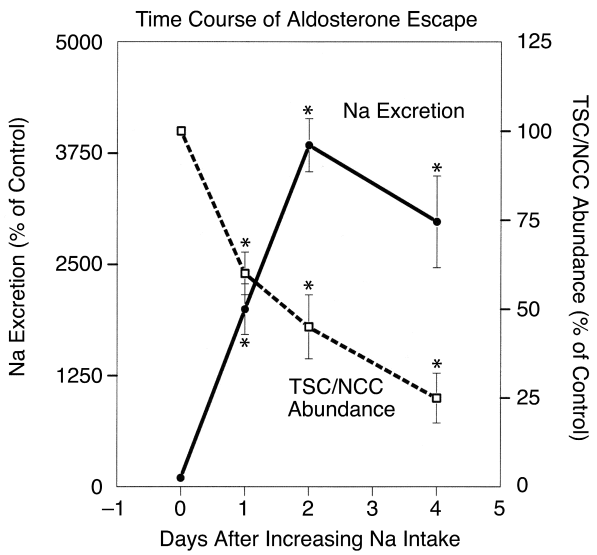

Figure 6
Time course of changes in NCC abundance and Na excretion after increase in NaCl intake in aldosterone-escape experiments. Experiments were conducted following the protocol shown in Figure 1. NCC abundance was assessed a relative band density in immunoblots as described above. *Significant difference relative to 0 day time point (before the increase in Na intake).

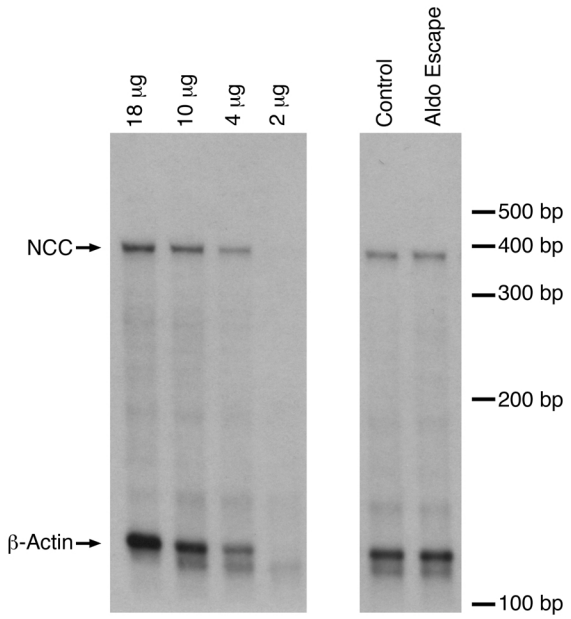

Figure 7
Assessment of NCC mRNA abundance in aldosterone-escape by RPA. Left: A titration series with 2–18 µg of renal cortical total RNA. NCC probe, 389 bp; β-actin probe, 127 bp. Right: Comparison of whole-kidney NCC mRNA abundance for a control rat versus an aldosterone-escape rat using 10 µg total RNA. Densitometric analysis of three pairs showed no significant difference in NCC mRNA between control and aldosterone-escape (see the text).

from the escape process by initiating the aldosterone infusion 3 days before a switch from a very low Na diet to a moderate-Na intake (2 mEq/d). The intake of food and water was carefully matched to avoid confounding variables. During the initial 3-day period, the high level of circulating aldosterone resulting from the infusion is appropriate for the low level of NaCl intake. Only after the NaCl intake is increased at day 0 is there a stimulus for the escape process.

Aldosterone escape is associated with a marked decrease in the abundance of the thiazide-sensitive Na-Cl cotransporter. The most striking finding of this study was a profound decrease in the amount of NCC protein, the target for the NaCl transport-inhibiting action of thiazide diuretic agents. The decrease occurred with a time course of onset that paralleled the increase in NaCl excretion associated with the escape process, and led to a fall in NCC protein abundance to 17–25% of baseline levels. The marked decrease in NCC abundance was confirmed by immunocytochemical observations, with no change in the distribution of NCC protein in the DCT cells. Micropuncture studies have revealed that the DCT, the site of NCC expression, normally absorbs at least 1–2% of the filtered load of Na in rats, and that the Na absorption is completely inhibited by chlorothiazide (23). In the present studies, Na excretion increased from about 0.02% of filtered load to 0.8% of filtered load during the escape process. Thus, the amount of Na absorption normally occurring in the DCT via NCC is sufficient, if fully inhibited, to account for the observed Na-excretion rate during the escape process.

In addition, there were effects on the γ subunit of ENaC, which may have contributed to the increase in Na excretion seen during the escape process. Specifically, there was a reduction in the amount of the 70-kDa form of γ-ENaC relative to the total. The formation of the 70-kDa form of γ-ENaC has been postulated to be due to a physiological proteolytic cleavage (4) by an extracellular serine protease called CAP1 (24). On the basis of studies demonstrating that extracellular application of trypsin increases the Na-transporting activity of ENaC heterologously expressed in *Xenopus* oocytes (25), we have proposed that formation of the 70-kDa form is associated with activation of ENaC in vivo (4). Based on the size of the product (70 kDa), the putative cleavage would have to occur in the early portion of the extracellular loop of γ-ENaC. In the present studies, aldosterone escape was associated with a reduction in the amount of the 70-kDa form, consistent with a reversal of the effects of aldosterone on the collecting duct principal cell. However, the other major effect of aldosterone, namely an increase in α subunit abundance, was not reversed during the escape process. Hence we believe it is unlikely that the escape process involves a general inhibition of aldosterone-mediated gene regulation. For example, it appears unlikely that the escape process could be due to a decrease in the abundance of the mineralocorticoid receptor. In addition, measurement of plasma aldosterone concentration did not reveal a significantly decreased level in the escape rats.

Based on experiments by Hall and his colleagues in which renal perfusion pressure was prevented from rising by a servo-null system (10), the aldosterone-escape process appears to depend on an increase in renal perfusion pressure. Thus, the aldosterone-escape phenomenon is presumably due to activation of long-term pressure natriuresis mechanisms. We speculate that pressure natriuresis may be multifactorial and may differ in character depending on the chronicity of the increase in arterial pressure. Pressure natriuresis has been studied most often in the context of acute increases in arterial blood pressure achieved by aortic clamping. Under these circumstances, pressure natriuresis appears to depend on inhibition of NaCl absorption in the proximal tubule, possibly by increased backleak of NaCl across the tight junctions (26) or as a result of endocytosis of Na transporters in the apical and basolateral plasma membranes of the proximal tubule (27). The changes found in the present study implicate additional mechanisms after a chronic stimulus to Na retention; namely, a marked decrease in NCC abundance in the distal convoluted tubule that could account for Na-excretion rates up to 2% of the filtered load. The effect on the thiazide-sensitive NaCl cotransporter is in accord with the findings of Majid and Navar indicating that, in contrast to findings with acute hypertension, long-term pressure natriuresis is dependent on inhibition of Na

transport in distal nephron segments (28). It is interesting that the marked suppression of NCC protein abundance occurred without a change in NCC mRNA level, indicating that the regulatory process is likely to involve changes in protein half-life or perhaps regulation of translation rate.

Proximal tubule Na transporters in aldosterone escape. These studies did not reveal changes in proximal tubule transporter expression that could explain aldosterone escape; in fact, the changes in proximal transporter abundances found are compatible with increased proximal NaCl absorption. Specifically, cortical Na-K-ATPase abundance was increased, presumably owing to an increase in the proximal tubule, the predominant tubule segment in the cortex. Furthermore, in whole-kidney samples, there were significant increases in the protein abundance of two proximal Na transporters, NHE3 and NaPi-2 (Table 2). Although these changes would predict increased proximal NaCl absorption, micropuncture studies have revealed that Na delivery to the early distal tubule is not decreased during aldosterone escape (11, 12). These observations would suggest that any increases in proximal tubule reabsorption during aldosterone escape are compensated for by decreases in Na absorption in the loop of Henle. Such a notion is compatible with the findings of studies in isolated perfused thick ascending limbs that showed that Na absorption increases or decreases as a direct function of the amount of Na delivered to the thick ascending limb, lowering the luminal Na concentration at the end of the cortical thick ascending limb to a relatively fixed value (29).

Acknowledgments

This study was funded by the Intramural Budget of the National Heart, Lung, and Blood Institute (NIH project Z01-HL-01282-KE to M.A. Knepper). Additional support for this study was provided by the Human Frontier Science Program, the Danish Medical Research Council, the Karen Elise Jensen Foundation, and the Commission of the European Union (EU-TMR Program). The authors thank Inger Merete Paulsen for expert technical assistance.

1. Bonvalet, J.P. 1998. Regulation of sodium transport by steroid hormones. *Kidney Int.* **65**:S49–S56.
2. Garty, H., and Palmer, L.G. 1997. Epithelial sodium channels: function, structure, and regulation. *Physiol. Rev.* **77**:359–396.
3. Canessa, C.M., et al. 1994. Amiloride-sensitive epithelial Na^+ channel is made of three homologous subunits. *Nature.* **367**:463–467.
4. Masilamani, S., Kim, G.-H., Mitchell, C., Wade, J.B., and Knepper, M.A. 1999. Aldosterone-mediated regulation of ENaC α, β, and γ subunit proteins in rat kidney. *J. Clin. Invest.* **104**:R19–R23.
5. Velazquez, H., Bartiss, A., Bernstein, P., and Ellison, D.H. 1996. Adrenal steroids stimulate thiazide-sensitive NaCl transport by rat renal distal tubules. *Am. J. Physiol.* **270**:F211–F219.
6. Kim, G.-H., et al. 1998. The thiazide-sensitive Na-Cl cotransporter is an aldosterone-induced protein. *Proc. Natl. Acad. Sci. USA.* **95**:14552–14557.
7. Relman, A.S., and Schwartz, W.S. 1952. The effect of DOCA on electrolyte balance in normal man and its relation to sodium chloride intake. *Yale J. Biol. Med.* **24**:540–558.
8. August, J.T., Nelson, D.H., and Thorn, G.W. 1958. Response of normal subjects to large amounts of aldosterone. *J. Clin. Invest.* **37**:1549–1555.
9. Young, W.F.J. 1999. Primary aldosteronism: a common and curable form of hypertension. *Cardiol. Rev.* **7**:207–214.
10. Hall, J.E., Granger, J.P., Smith, M.J., and Premen, A.J. 1984. Role of renal hemodynamics and arterial pressure in aldosterone "escape". *Hypertension.* **6**:I183–I192.
11. Haas, J.A., Berndt, T.J., Youngberg, S.P., and Knox, F.G. 1979. Collecting duct sodium reabsorption in deoxycorticosterone-treated rats. *J. Clin. Invest.* **63**:211–214.
12. Kohan, D.E., and Knox, F.G. 1980. Localization of the nephron sites responsible for mineralocorticoid escape in rats. *Am. J. Physiol.* **239**:F149–F153.
13. Brooks, H.L., et al. 2001. Profiling of renal tubule Na^+ transporter abundances in NHE3 and NCC null mice using targeted proteomics. *J. Physiol.* **530**:359–366.
14. Kim, G.-H., et al. 2000. Long-term regulation of sodium-dependent cotransporters and ENaC in rat kidney: response to altered acid-base intake. *Am. J. Physiol.* **279**:F459–F467.
15. Fernandez-Llama, P., Andrews, P., Ecelbarger, C.A., Nielsen, S., and Knepper, M.A. 1998. Concentrating defect in experimental nephrotic syndrome: altered expression of aquaporins and thick ascending limb Na^+ transporters. *Kidney Int.* **54**:170–179.
16. Kim, G.-H., et al. 1999. Vasopressin increases Na-K-2Cl cotransporter expression in thick ascending limb of Henle's loop. *Am. J. Physiol.* **276**:F96–F103.
17. Terris, J., Ecelbarger, C.A., Nielsen, S., and Knepper, M.A. 1996. Long-term regulation of four renal aquaporins in rat. *Am. J. Physiol.* **271**:F414–F422.
18. Ecelbarger, C.A., et al. 1997. Role of renal aquaporins in escape from vasopressin-induced antidiuresis in rat. *J. Clin. Invest.* **99**:1852–1863.
19. Hager, H., et al. 2001. Immunocytochemical and immunoelectron microscopical localization of α-, β- and γ-ENaC in rat kidney. *Am. J. Physiol. Renal Physiol.* **280**:F1093–F1106.
20. Chomczynski, P., and Sacchi, N. 1987. Single-step method of RNA isolation by acid guanidinium thiocyanate-phenol-chloroform extraction. *Anal. Biochem.* **162**:156–159.
21. Plotkin, M.D., et al. 1996. Localization of the thiazide sensitive Na-Cl cotransporter, rTSC1 in the rat kidney. *Kidney Int.* **50**:174–183.
22. Ecelbarger, C.A., et al. 1996. Localization and regulation of the rat renal Na^+-K^+-$2Cl^-$ cotransporter, BSC-1. *Am. J. Physiol.* **271**:F619–F628.
23. Ellison, D.H., Velazquez, H., and Wright, F.S. 1987. Thiazide-sensitive sodium chloride cotransport in early distal tubule. *Am. J. Physiol.* **253**:F546–F554.
24. Vallet, V., Chraibi, A., Gaeggeler, H.P., Horisberger, J.D., and Rossier, B.C. 1997. An epithelial serine protease activates the amiloride-sensitive sodium channel. *Nature.* **389**:607–610.
25. Chraibi, A., Vallet, V., Firsov, D., Hess, S.K., and Horisberger, J.D. 1998. Protease modulation of the activity of the epithelial sodium channel expressed in Xenopus oocytes. *J. Gen. Physiol.* **111**:127–138.
26. Knox, F.G., and Granger, J.P. 1992. Control of sodium excretion: an integrative approach. In *Handbook of physiology: renal physiology*. E.E. Windhager, editor. Oxford University Press. New York, New York, USA. 927–967.
27. Zhang, Y., et al. 1996. Rapid redistribution and inhibition of renal sodium transporters during acute pressure natriuresis. *Am. J. Physiol.* **270**:F1004–F1014.
28. Majid, D.S., and Navar, L.G. 1994. Blockade of distal nephron sodium transport attenuates pressure natriuresis in dogs. *Hypertension.* **23**:1040–1045.
29. Burg, M.B. 1982. Thick ascending limb of Henle's loop. *Kidney Int.* **22**:454–464.